UNIVERSITÉ DE GENÈVE

Archive ouverte UNIGE
https://archive-ouverte.unige.ch

Article scientifique | Article | 2018

Accepted version | Open Access

This is an author manuscript post-peer-reviewing (accepted version) of the original publication. The layout of the published version may differ .

Double-Stranded RNA-Specific Templated Reaction with Triplex Forming PNA

Kim, Kitae; Chang, Dalu; Winssinger, Nicolas

How to cite

KIM, Kitae, CHANG, Dalu, WINSSINGER, Nicolas. Double-Stranded RNA-Specific Templated Reaction with Triplex Forming PNA. In: Helvetica Chimica Acta, 2018, vol. 101, n° 3, p. e1700295. doi: 10.1002/hlca.201700295

This publication URL: https://archive-ouverte.unige.ch//unige:103235
Publication DOI: 10.1002/hlca.201700295

© This document is protected by copyright. Please refer to copyright holder(s) for terms of use.

Double-Stranded RNA-specific Templated Reaction with Triplex Forming PNA

Ki Tae Kim, Dalu Chang, and Nicolas Winssinger *,

Department of Organic Chemistry, NCCR Chemical Biology, Faculty of Science, University of Geneva, 30 quai Ernest Ansermet, 1211 Geneva, Switzerland.

ABSTRACT: RNA, originally perceived as a simple information transfer biopolymer, is emerging as an important regulator in cellular processes. A number of non-coding RNAs are double-stranded and there is a need for technologies to reliably detect and image such RNAs for biological and biomedical research. Herein we report double-stranded RNA-specific templated reaction resulting from PNA-reagent conjugates that are brought within reactive distance through the formation of sequence-specific triplexes onto double-stranded RNA. The reaction makes use of a ruthenium-based photocatalyst that reduces a pyridinium-based immolative linker, unmasking a profluorophore. The reaction was shown to proceed with signal amplification and to be selective for double-stranded RNA over DNA as well as single-stranded RNA. The generality of the triplex formation was enabled by non-canonical nucleobases that extend the Hoogsteen base-pairing repertoire. The technology was applied to a templated reaction using pre-microRNA 31.

Keywords: Templated reaction • supramolecular chemistry • PNA • dsRNA • miR

Introduction

The past decades have brought a paradigm shift regarding the role of RNA with accumulating evidence that its functions extend far beyond simple messaging between DNA and proteins.[1] Only 3 % of our genome encodes proteins, yet the work that emerged from the Encyclopedia of DNA Elements (ENCODE) project[2] revealed that 76% of the genome is transcribed, bolstering the notion that an important portion of non-coding RNA (ncRNA) has a role. Non-coding RNA (ncRNA) genes yield functional RNAs rather than proteins, with important function in directing post-translational regulation of gene expression and RNA modifications. [3] Double-stranded RNA (dsRNA) has emerged as an important regulator of gene expression in many eukaryotes. It triggers different types of gene silencing that are collectively referred to as RNA silencing or RNA interference .[4] Such ncRNAs are typically regulated by a complex set of modifications and understanding their biogenesis is crucial.[5, 6] As a single strand biopolymer, RNA tends to adopt diverse intermolecular folds with stretches of dsRNA.[7] MicroRNAs (miRs) which, in their mature form are approximately 21 nt, are processed from larger double-stranded precursors following a choreographed series of events. [8, 9] These advances have transformed our appreciation for the tremendous number, diversity and biological importance of ncRNAs. Accordingly, technologies to sense and interfere with ncRNAs are important.[10] Recently, triplex-forming PNAs with a fluorogen as a base surrogate were reported as a turn-on probe for dsRNA. [11, 12] Oligonucleotide-templated reactions have emerged as a powerful technology to sense and image ssDNA or RNA.[13-17] Oligonucleotide-templated reactions are promoted by the high effective concentration achieved following hybridization of the reagent conjugates. These reactions have been shown to be possible in a cellular context as well as live organisms[18] and can be used to unmask fluorophores or bioactive compounds.[19-21] Templated reactions have the potential to turnover and provide signal amplification. Proteins have also been used to template reactions using the same concept of proximity-induced reactions.[22-24] Herein we extend this chemistry to dsRNA and demonstrate that the reaction is specific to a dsRNA over dsDNA or ssRNA (Fig. 1).

While peptide nucleic acids (PNAs) are known to form triplex with DNA,[25] such triplex formations are restricted to purine sequences using the canonical nucleobases and proceed under specific conditions (low salt, acidic pH). Recently, Rozner and coworkers extended the scope of triplex forming PNA with the introduction of monomers bearing novel nucleobases that extend the Hoogsteen triplex base-pairing[26] to any sequence permutation (M•G-C, P•C-G, E•U-A, Fig. 1) and showed that triplex formation was selective for dsRNA over dsDNA.[27-30] The fact that the M nucleobase is more basic than the C nucleobase also enables triplex formation at higher pH, at or near physiological conditions.

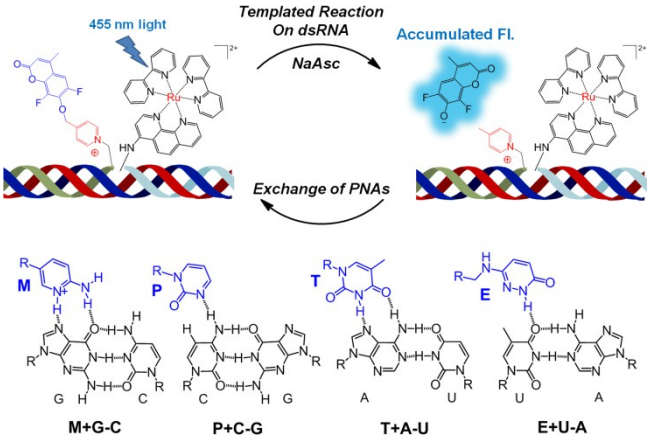

Figure 1. Top: Schematic representation of dsRNA templated reaction between Ru(bpy)$_2$phen or pyridinium coumarin (PyCou) based on triplex formation leading the accumulation of fluorophore (Fl); Bottom: Chemical structures and Hoogsteen hydrogen-bonding patterns of modified nucleobases M, P, and E designed to recognize the G-C, C-G, and U-A nucleobases, respectively, as well as T which pairs A-U for a PNA-dsRNA triplex.

Results and Discussion

Design of dsRNA templated reaction

We began our work with a dsRNA derived from sequences that have been productively used in hybridization chain reaction (HCR).[31] As shown in Fig. 1; two PNA probes conjugated to the ruthenium-based photocatalyst and the pyridinium-based immolative linker, respectively, are required. Triplex formation brings the ruthenium-based photocatalyst (Ru(bpy)$_2$phen) within reactive distance of the pyridinium-based immolative linker. Photoexcitation of the catalyst using a 455 nm LED lamp followed by ascorbate reduction yields a reduced ruthenium catalyst that transfers an electron to the pyridinium resulting in an elimination of the benzylic substituent (immolation). We opted for difluorocoumarin as the leaving group based on the fact that it had been successfully used in the templated reaction previously, yielding a fluorogenic signal that is spectrally resolved from the ruthenium photocatalyst.[32] The design of the probes was made with the following considerations: each probe should use a different strand of the duplex to minimize any background reaction arising from ssRNA-templated reaction; sequences rich in M and T monomers will form more stable triplex; 8-mer probes should achieve the necessary affinity to yield a templated reaction at low concentration (less than100 nM); the reagents should be separated from the PNA with a short polyethylene glycol spacer (PEG: 9 atoms) to relieve any unfavorable conformational bias. Based on these considerations a set of probes was designed as shown in Fig. 2. The ruthenium photocatalyst-conjugate probe (**Ru1**) interacts with **RNA 1** of the **RNA1**:**RNA2** duplex, whereas the coumarin-conjugate probes (**Cou1**-**3**) interact with **RNA2** of the same duplex. Three different coumarin-conjugate probes were prepared in order to vary the distance between the reaction sites.

The reactions were monitored through the increase of fluorescence arising from the unmasking of coumarin as a function of time. Using optimal conditions for triplex formation (pH 6.85, HEPES-KOH buffer, 50 mM NaCl) and performing the reaction at 100 nM of probes with stoichiometric template, we were pleased to observe a dsRNA-specific reaction (Fig. 2a). The reaction of **Ru1** and **Cou1** proceeded significantly faster in the presence of dsRNA than with either of the single strand RNA (**RNA1** or **RNA2**). Comparing the initial speed of the reaction from the slope of the reaction after 10 min, the dsRNA was 7 times faster than either single strand RNA and 71 times faster than the background reaction lacking RNA template. It is noteworthy that the high selectivity for dsRNA *vs* single strand RNA templated reaction is dependent on the salt concentration; in the absence of NaCl, the reaction of dsRNA was only 2-fold faster than ssRNA (see Fig. S1, A). At concentration of NaCl above 50 mM, the reaction had comparable performance as 50 mM but with slower kinetics (Fig. S1 B and C for 60 and 70 mM NaCl, respectively). Importantly, the reaction also afforded good discrimination between dsRNA and ssRNA template in PBS buffer (Fig. S1 D).

We next compared the reactivity of coumarin probes leaving a single or double base-pair gap between the probes forming the triplex (**Cou2** and **Cou3** respectively). Both of these reactions proved to be almost twice as fast compared to the reaction of **Cou1** + **Ru1** (Fig. 2 B and C), with an initial rate of reaction that is over 10-fold faster for dsRNA than the reaction with either ssRNAs. A dsDNA template with the same sequence as **RNA1** + **RNA2** did not catalyze the reaction, nor did either of the ssDNA template (Fig. 2C). Assuming a quantitative formation of the quaternary complex of the dsRNA with the two probes forming the triplex, the reaction is anticipated to follow a first order kinetics and the half-life of the reaction can be used to derive a pseudo first-order rate constant. Following this analysis, rates of 0.44 x 10^{-3} to 0.89 x 10^{-3} s^{-1} were measured for the different reactions (Fig. 1D). Comparing the sequence of **Cou1** vs **Cou2**, they

have the same nucleobase content, suggesting that the 2-fold kinetic difference observed between the reactions of **Ru1** with **Cou1** vs **Cou2** is the fact that there is a more favorable reagent alignment in the latter reaction. Another possible explanation is the fact that adjacent M nucleobases at the junction of **Cou1** and **Ru1** triplex with protonated amino pyridines result in a distortion that is slightly detrimental to the reaction kinetics. The same dependence of NaCl concentration was observed for the reaction of **Cou3** and **Ru1** as with **Cou1** and **Ru1** with respect to the selectivity of dsRNA templated reaction vs ssRNA templated reaction. Namely, 50 mM NaCl, or higher concentrations, is important to achieve good selectivity of dsRNA vs ssRNA (Fig. S2 A,B). Importantly, the reaction of **Cou3** with **Ru1** proceeded equally at pH 7.4 with a high selectivity for dsRNA (Fig. S2 C,D). Performing the reaction at different concentrations (100 – 400 nM) did not have a strong influence on the reaction kinetics suggesting that indeed, the quaternary complex is formed quantitatively under these conditions (Fig. S3).

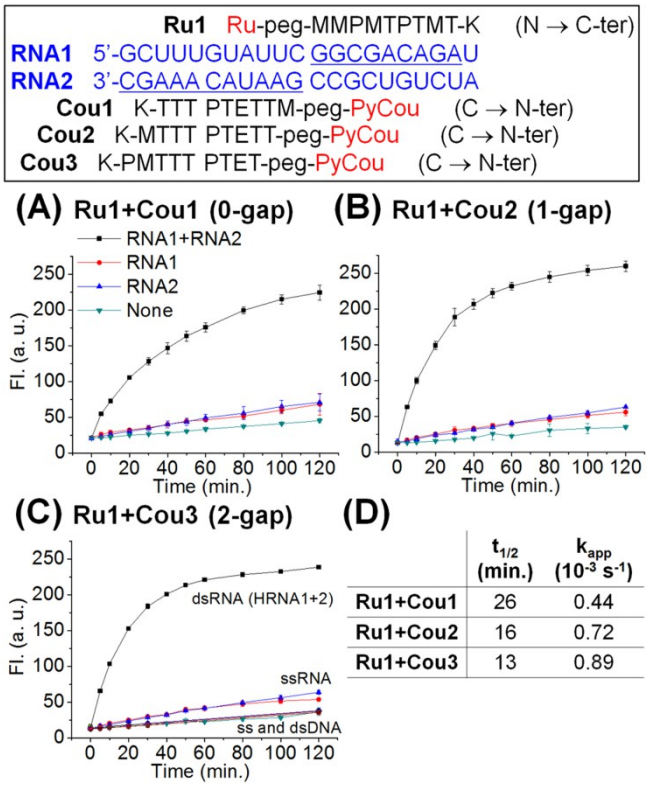

	$t_{1/2}$ (min.)	k_{app} (10^{-3} s^{-1})
Ru1+Cou1	26	0.44
Ru1+Cou2	16	0.72
Ru1+Cou3	13	0.89

Figure 2. Top: RNA sequences used and alignment of the PNA probes (see SI for explicit structures); (A) **Ru1+Cou1**, (B) **Ru1+Cou2**, and (C) **Ru1+Cou3** in the presence of **RNA1+RNA2**, **RNA1**, **RNA2**, or none. peg = [(aminoethoxy)ethoxy] acetic acid, K = lysine. Reaction condition: 100 nM of PNAs and 100 nM of ss or dsRNAs, 30 mM HEPES-KOH pH 6.85, 50 mM NaCl, 5 mM sodium ascorbate, 0.02 % Tween-20; (D) Measured half-life and k_{app} of the templated reactions.

We then evaluated the performance of the reaction using sub-stoichiometric quantities of template in order to achieve signal amplification. Using 20% dsRNA, the yield of product exceeded template loading within less than 20 min of reaction and reached 76% completion within 2h (Fig. 3 A). Under these conditions, the reaction retained the same discrimination for dsRNA over either of the ssRNA. Reducing the concentration of dsRNA to 5 nM (0.02 equivalent of template) and 0.5 nM (0.002 equivalent of template) still afforded reaction discernable over background. Running the reaction for 7h afforded a total conversion of 68 % conversion with 0.02 equivalent of the template. Adjusting for the background reaction, this corresponds a 19-fold signal amplification (37 % yield, 19 turnovers). The reaction with 0.5 nM template afforded 3 % yield (adjusting for the background conversion) after 7h, representing 15-fold signal amplification. It should be noted that the rate of triplex formation (10^3 to 10^4 $M^{-1}s^{-1}$)[33] is known to be slower than hybridization of a duplex (10^6 $M^{-1}s^{-1}$).[32] We have recently shown that templated reactions engineered to yield a product with lower affinity for the template enhances the turnover of the reaction, provided reagent dissociation is rate-limiting.[34] However, in the present case, the reaction is the rate-limiting step.

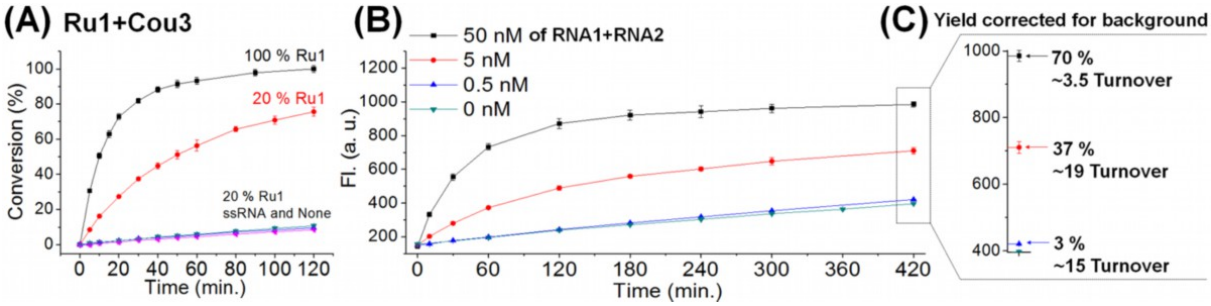

Figure 3. (A) Plot of the conversion for the templated reaction of **Cou3** (250 nM) with 1 eq. (250 nM, black line) or 0.2 eq. of **Ru1** (50 nM, red line) in the presence of 0.2 eq. (50 nM) of dsRNA (**RNA1+RNA2**) or ssRNA; (B) Plot of the conversion for the reaction at various template (dsRNA: **RNA1+RNA2**) loading; (C) Calculated yield and turnovers for the reactions (the yield was obtained by subtracting the conversion observed in the presence and absence of template). Reaction condition: 30 mM HEPES-KOH pH 6.85, 50 mM NaCl, 5 mM sodium ascorbate, 0.02 % Tween-20. Yields are calculated based on a titration of the coumarin, see SI for details.

The number of M nucleobases in a given PNA probe dictates the number of cationic charges and this has a strong impact on the overall affinity and kinetics of the triplex formation; in particular at higher NaCl concentrations.[33] The ruthenium photocatalyst further adds two cationic charges to the PNA probes. Analysis of the sequences used in the reactions shown above revealed that the **Ru1** sequence (7 charges) was overall more cationic than the **Cou1**-**3** sequences (3-4 charges). By switching the position of the photocatalyst and pyridinium-coumarin, we would alter the charge balance without changing the overall PNA sequences . Thus **Ru2** and **Cou4** probes were prepared and their performance in templated reactions studied (Fig. 4). Interestingly, the reaction was found to be more resilient to high salt concentration and still afforded signal at 150 mM NaCl. Under the same conditions, **Ru1** and **Cou3** (same PNA sequences but opposite position of photocatalyst and pyridinium-coumarin conjugate) did not afford reaction pointing to the importance of the overall cationic charges for the triplex formation at high salt concentrations. The reaction was specific for the sequence of dsRNA, a mismatched sequence was comparable to no template (Fig. 4B). Increasing the length of the PEG linker (from 9 atoms to 18 atoms) between the PNA and reagents (ruthenium photocatalyst and pyridinium-coumarin conjugate) did not have a significant impact on the reaction kinetics (Fig. S4A). PNAs modified at the γ position(*L* stereochemistry) have been reported to enhance duplex stability and induce a helical preorganization of PNAs.[35] Using a γ-modified PNA with serine side chains,[36] we tested the reaction with the same sequence as **Ru2** and **Cou4** wherein four and three of the positions, respectively, contained a γ-modification. Templated reaction using dsRNA showed slower reaction for the probes with γ-modified PNAs suggesting that such modifications are detrimental to the triplex formation (Fig. S4B).

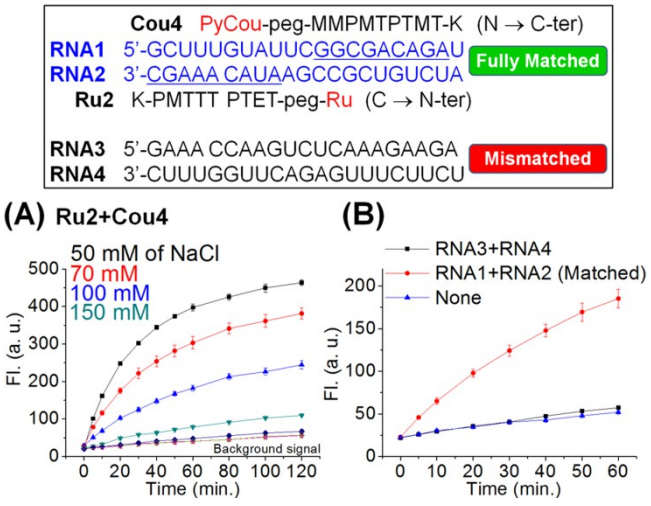

Figure 4. (A) Templated reaction of **Ru2+Cou4** in the presence of **RNA1+RNA2** with different concentration of NaCl (background signal is from ssRNA or none); (B) templated reaction of **Ru2+Cou4** in the presence of fully matched dsRNA (**RNA1+RNA2**) or mismatched dsRNA sequence (**RNA3+RNA4**) in 100 mM NaCl concentration. Reaction condition: 100nM of PNAs and 100 nM of ss or dsRNAs, 30 mM pH 6.85 HEPES-KOH, 5 mM sodium ascorbate, 0.02 % Tween-20, incubation time: 30 min.

Detection of pre-miR-31 sequence using dsRNA-templated reaction

Based on the successful design of templated reactions responding to dsRNA, we turned our attention to the application of this technology for the detection of pre-microRNA sequences, an important class of ncRNA. Pre-microRNAs are well-known to regulate expression, serving

as endogenous antisense agents.[37, 38] As a target sequence, we chose pre-miR-31 based on the fact that its abundance correlates to the function of the p53 pathway, an important tumor suppressor pathway.[9, 39] Selective detection of pre-miR-31 is important because there is a significant discrepancy between the level of pre-miR (as high as 10 000 copies/ cell) and the mature miR in several cancer cell lines.[8, 40] Based on the structure of the 71-mer pre-miR-31 hairpin sequence, we used two fragments of this 71-mer (miR-31-5p and miR-31-3p) in order to assess the discrimination between dsRNA vs ssRNA detection (Fig. 5). We designed PNAs keeping in mind that the PNA should have: i) at least 9-mer and four M monomer to have strong binding to dsRNA; ii) 1-3 cationic amino acids in the sequence to overcome the destabilization incurred by high salt concentrations; iii) the strand affording the more stable triplex should be used since the pre-miR-31 has several bulges in the dsRNA stretches. According to these considerations, several possible binding sites in pre-miR-31 for the PNA were identified (Fig. 5).

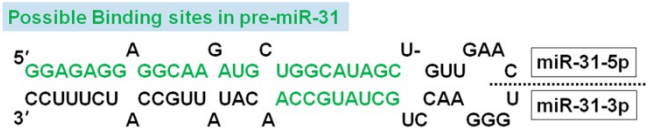

Figure 5. The structure of pre-miR-31hairpin (71-mer) and possible binding site for PNAs. Pre-miR-31 was divided into two parts, miR-31-5p and -3p sequences for this work.

We first synthesized **5pRu1** (11-mer PNA, 5 Ms, 2 Lys, 9 cationic charges) and **5pCou1** (13-mer PNA, 4 Ms, 3 Lys, 8 cationic charges). The templated reaction between **5pRu1** and **5pCou1** yielded strong fluorescence enhancements in the presence of pre-miR-31 at different NaCl concentrations ranging from 50 to 150 mM (Fig. 6 and S5 and S6). However, we also observed a weak signal in the presence of the ssRNA template (miR-31-5p). Efforts to suppress this background reaction with an alternative pyridinium coumarin probe (**5pCou2**, 13-mer PNA, 5 Ms, 3 Lys, 9 cationic charges, Fig. 6B and S7), and the number of lysines (**5pCou4**, 13-mer PNA, 5 Ms, 0 Lys, 6 cationic charges, Fig. S8), still resulted in a partial response to ssRNA miR-31-5p. The PNA sequences in the present case were made longer than in the previous case (Fig. 2-4) to accommodate the bulges in the pre-miR-31. We speculated that this longer PNA retained sufficient duplex stability with ssRNA to yield a templated reaction under these conditions. We next investigated probes designed to have 9-mer PNA with 7 cationic charges and to be positioned in the middle of pre-miR-31. From this, two PNAs, **5pCou3** (9-mer PNA, 4 Ms, 2 Lys, 7 cationic charge) and **5pRu2** (9-mer PNA, 3 Ms, 2 Lys, 7 cationic charge) were prepared and tested (Fig. 6 C and D). **5pRu2**+**5pCou3** exhibited clear discrimination between the dsRNA (pre-miR-31) and the ssRNA fragment (miR-31-p) at physiological salt concentrations (Fig. 6C). Concurring previous reactions, lower NaCl concentrations resulted in poorer selectivity (Fig. S9). It is noteworthy that using the miR-31-3p strand with the dsRNA complex for templated reaction afforded poorer results and did not proceed at 100 mM NaCl (Fig. S10 and S11). This result clearly highlights that the choice in the templating strand for the triplex is critical to the success of the reaction. While it is generally preferable to use to different strand for each probe to minimize the potential for background reaction arising from ssRNA template (design used in Figs. 2-4); it is possible to achieve dsRNA specific reaction with probes targeting the same strand. The choice of which templating strand to use should be dictated by the number of M nucleobases to be included in the probe.

Finally, we tested templated reaction of **5pCou3** and catalytic amount of **5pRu2** in the presence of different amount of pre-miR-31 samples to assess the detection range of the system. We have used 250 nM of **5pCou3** and 20 % of **5pRu2** (50 nM) to monitor concentration dependency of this catalytic templated reaction (Fig. 6D). Even at 12.5 nM of a target sample, a distinguishable signal was obtained after 30 min, which implies practical detection of pre-miR-31 at low nanomolar concentration.

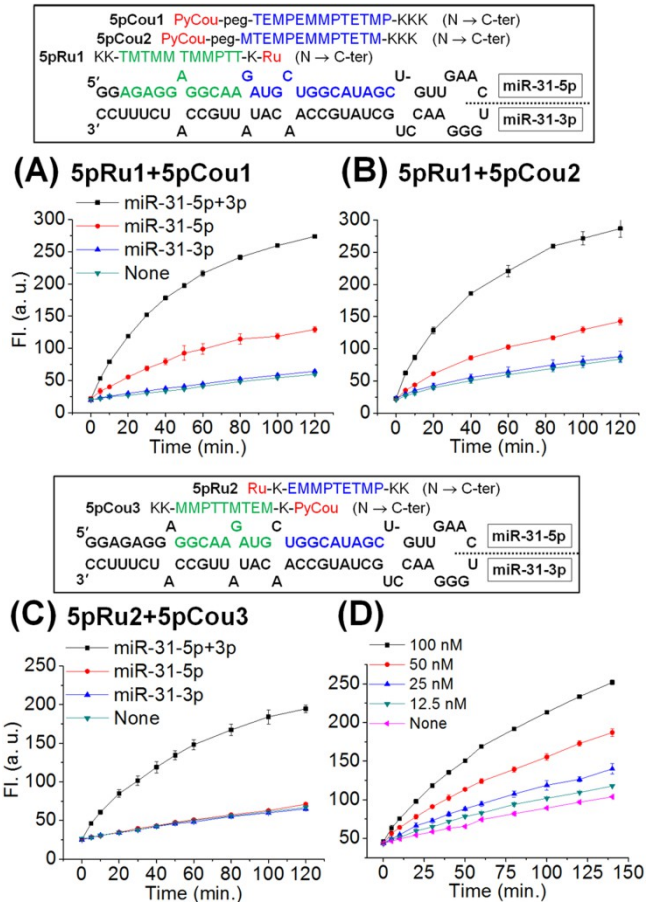

Figure 6. One-to-one templated reaction of (A) **5pRu1+5pCou1** (100 nM), (B) **5pRu1+5pCou2** (100 nM), and (C) **5pRu2+5pCou3** (100 nM) in the presence of the duplex or single strand form of mir-31-5p and 3p (100 nM); (D) Templated reaction between **5pRu2** (50 nM) and **5pCou3** (250 nM) in the presence of 12.5-100 nM of pre-miR-31 duplexes formed by miR-31-5p and 3p. Conditions: 1´PBS buffer, 0.02 % tween-20, 5 mM sodium ascorbate, 140 min. of reaction time, 1% of sperm DNA.

Conclusions

We have developed a dsRNA-selective templated reaction based on triplex formation between dsRNA and PNAs modified with M, P, and E nucleobases. An important design consideration to achieve high discrimination between dsRNA and ssRNA is the length of the PNA probe and the number of M nucleobases. It is important to note that the reactions are very selective for dsRNA vs dsDNA in agreement with the fact that PNAs form more stable triplex with dsRNA than dsDNA. While γ-modified PNAs have been shown to enhance duplex stability, this modification was found to be detrimental to triplex formation. These findings extend the utility of templated reactions to an important nucleic acid motif in biology and were shown to be applicable to a representative pre-miR. The presence of at least two bulges in the dsRNA stretch was tolerated in the dsRNA-templated reaction. As for other templated reactions, we showed that a dsRNA can yield a signal amplification of nearly 20-fold.

Experimental Section

See supplementary Material

Supplementary Material

General experimental details including synthetic procedures of PNA strands and sample preparation for templated reaction, sequence information of PNAs and RNAs, kinetic data, fluorescence spectra, MALDI-TOF, and LC-MS data are available as part of supporting information. Supporting information for this article is available on the WWW under http://dx.doi.org/10.1002/MS-number.

Acknowledgements

The authors thank the SNSF (grant: 200020_157106) and the NCCR Chemical Biology for financial support.

Author Contribution Statement.

KTK, DC NW designed the experiments and analyzed the data. KTK and DC performed the synthesis of all the probes used in this study and ran the templated reaction and their kinetic analysis.

REFERENCES

[1] K. V. Morris, J. S. Mattick, 'The rise of regulatory RNA', *Nat. Rev. Genet.* **2014**, *15*, 423-437.
[2] E. Pennisi, 'Genomics. ENCODE project writes eulogy for junk DNA', *Science* **2012**, *337*, 1159, 1161.
[3] S. R. Eddy, 'Non-coding RNA genes and the modern RNA world', *Nat. Rev. Genet.* **2001**, *2*, 919-929.
[4] G. Meister, T. Tuschl, 'Mechanisms of gene silencing by double-stranded RNA', *Nature* **2004**, *431*, 343-349.
[5] E. Lund, S. Guttinger, A. Calado, J. E. Dahlberg, U. Kutay, 'Nuclear export of microRNA precursors', *Science* **2004**, *303*, 95-98.
[6] A. G. Matera, R. M. Terns, M. P. Terns, 'Non-coding RNAs: lessons from the small nuclear and small nucleolar RNAs', *Nat. Rev. Mol. Cell Biol.* **2007**, *8*, 209-220.
[7] J. A. Cruz, E. Westhof, 'The dynamic landscapes of RNA architecture', *Cell* **2009**, *136*, 604-609.
[8] T. D. Schmittgen, 'Regulation of microRNA processing in development, differentiation and cancer', *J. Cell Mol. Med.* **2008**, *12*, 1811-1819.
[9] C. J. Creighton, M. D. Fountain, Z. Yu, A. K. Nagaraja, H. Zhu, M. Khan, E. Olokpa, A. Zariff, P. H. Gunaratne, M. M. Matzuk, M. L. Anderson, 'Molecular profiling uncovers a p53-associated role for microRNA-31 in inhibiting the proliferation of serous ovarian carcinomas and other cancers', *Cancer Res.* **2010**, *70*, 1906-1915.
[10] M. D. Disney, A. J. Angelbello, 'Rational Design of Small Molecules Targeting Oncogenic Noncoding RNAs from Sequence', *Acc. Chem. Res.* **2016**, *49*, 2698-2704.
[11] T. Sato, Y. Sato, S. Nishizawa, 'Triplex-Forming Peptide Nucleic Acid Probe Having Thiazole Orange as a Base Surrogate for Fluorescence Sensing of Double-stranded RNA', *J. Am. Chem. Soc.* **2016**, *138*, 9397-9400.
[12] T. Chiba, T. Sato, Y. Sato, S. Nishizawa, 'Red-emissive triplex-forming PNA probes carrying cyanine base surrogates for fluorescence sensing of double-stranded RNA', *Org. Biomol. Chem.* **2017**, *15*, 7765-7769.
[13] A. P. Silverman, E. T. Kool, 'Detecting RNA and DNA with templated chemical reactions', *Chem. Rev.* **2006**, *106*, 3775-3789.
[14] K. Gorska, N. Winssinger, 'Reactions Templated by Nucleic Acids: More Ways to Translate Oligonucleotide-Based Instructions into Emerging Function', *Angew. Chem. Int. Ed.* **2013**, *52*, 6820-6843.
[15] C. Percivalle, J. F. Bartolo, S. Ladame, 'Oligonucleotide-templated chemical reactions: pushing the boundaries of a nature-inspired process', *Org. Biomol. Chem.* **2013**, *11*, 16-26.
[16] M. Di Pisa, O. Seitz, 'Nucleic Acid Templated Reactions for Chemical Biology', *ChemMedChem* **2017**, *12*, 872-882.
[17] S. Barluenga, N. Winssinger, 'PNA as a Biosupramolecular Tag for Programmable Assemblies and Reactions', *Acc Chem Res* **2015**, *48*, 1319-1331.
[18] L. Holtzer, I. Oleinich, M. Anzola, E. Lindberg, K. K. Sadhu, M. Gonzalez-Gaitan, N. Winssinger, 'Nucleic Acid Templated Chemical Reaction in a Live Vertebrate', *ACS Cent. Sci.* **2016**, *2*, 394-400.
[19] A. Shibata, Y. Ito, H. Abe, 'RNA-templated molecule release induced protein expression in bacterial cells', *Chem. Commun.* **2013**, *49*, 270-272.
[20] A. Erben, T. N. Grossmann, O. Seitz, 'DNA-triggered synthesis and bioactivity of proapoptotic peptides', *Angew. Chem. Int. Ed.* **2011**, *50*, 2828-2832.
[21] K. Gorska, A. Manicardi, S. Barluenga, N. Winssinger, 'DNA-templated release of functional molecules with an azide-reduction-triggered immolative linker', *Chem. Commun.* **2011**, *47*, 4364-4366.
[22] N. Brauckhoff, G. Hahne, J. T. Yeh, T. N. Grossmann, 'Protein-templated peptide ligation', *Angew. Chem. Int. Ed.* **2014**, *53*, 4337-4340.
[23] J. Saarbach, E. Lindberg, S. Folliet, S. Georgeon, O. Hantschel, N. Winssinger, 'Kinase-templated abiotic reaction', *Chem. Sci.* **2017**, *8*, 5119-5125.
[24] K. K. Sadhu, T. Eierhoff, W. Römer, N. Winssinger, 'Photoreductive Uncaging of Fluorophore in Response to Protein Oligomers by Templated Reaction in Vitro and in Cellulo', *J. Am. Chem. Soc.* **2012**, *134*, 20013-20016.
[25] M. Egholm, P. E. Nielsen, O. Buchardt, R. H. Berg, 'RECOGNITION OF GUANINE AND ADENINE IN DNA BY CYTOSINE AND THYMINE CONTAINING PEPTIDE NUCLEIC-ACIDS (PNA)', *J. Am. Chem. Soc.* **1992**, *114*, 9677-9678.
[26] S. Hildbrand, A. Blaser, S. P. Parel, C. J. Leumann, '5-substituted 2-aminopyridine C-nucleosides as protonated cytidine equivalents: Increasing efficiency and selectivity in DNA triple-helix formation', *J. Am. Chem. Soc.* **1997**, *119*, 5499-5511.
[27] T. Zengeya, P. Gupta, E. Rozners, 'Triple-Helical Recognition of RNA Using 2-Aminopyridine-Modified PNA at Physiologically Relevant Conditions', *Angew. Chem. Int. Ed.* **2012**, *51*, 12593-12596.
[28] O. Muse, T. Zengeya, J. Mwaura, D. Hnedzko, D. W. McGee, C. T. Grewer, E. Rozners, 'Sequence Selective Recognition of Double-Stranded RNA at Physiologically Relevant Conditions Using PNA-Peptide Conjugates', *ACS Chem.Biol.* **2013**, *8*, 1683-1686.
[29] D. Hnedzko, S. K. Cheruiyot, E. Rozners, 'Using triple-helix-forming Peptide nucleic acids for sequence-selective recognition of double-stranded RNA', *Curr. Protoc. Nucleic Acid Chem.* **2014**, *58*, 4 60 61-23.
[30] T. Endoh, D. Hnedzko, E. Rozners, N. Sugimoto, 'Nucleobase-Modified PNA Suppresses Translation by Forming a Triple Helix with a Hairpin Structure in mRNA In Vitro and in Cells', *Angew. Chem. Int. Ed.* **2016**, *55*, 899-903.
[31] H. M. Choi, J. Y. Chang, A. Trinh le, J. E. Padilla, S. E. Fraser, N. A. Pierce, 'Programmable in situ amplification for multiplexed imaging of mRNA expression', *Nat Biotechnol* **2010**, *28*, 1208-1212.
[32] D. Chang, E. Lindberg, N. Winssinger, 'Critical Analysis of Rate Constants and Turnover Frequency in Nucleic Acid-Templated Reactions: Reaching Terminal Velocity', *J. Am. Chem. Soc.* **2017**, *139*, 1444-1447.
[33] D. Hnedzko, D. W. McGee, Y. A. Karamitas, E. Rozners, 'Sequence-selective recognition of double-stranded RNA and enhanced cellular uptake of cationic nucleobase and backbone-modified peptide nucleic acids', *RNA* **2017**, *23*, 58-69.
[34] D. Chang, K. T. Kim, E. Lindberg, N. Winssinger, 'Accelerating Turnover Frequency in Nucleic Acid Templated Reactions', *Bioconjug. Chem.* **2018**, *29*, 158-163.

[35] A. Dragulescu-Andrasi, S. Rapireddy, B. M. Frezza, C. Gayathri, R. R. Gil, D. H. Ly, 'A simple gamma-backbone modification preorganizes peptide nucleic acid into a helical structure', *J. Am. Chem. Soc.* **2006**, *128*, 10258-10267.

[36] D. Chouikhi, M. Ciobanu, C. Zambaldo, V. Duplan, S. Barluenga, N. Winssinger, 'Expanding the Scope of PNA-Encoded Synthesis (PES): Mtt-Protected PNA Fully Orthogonal to Fmoc Chemistry and a Broad Array of Robust Diversity-Generating Reactions', *Chem. Eur. J.* **2012**, *18*, 12698-12704.

[37] H. Dong, J. Lei, L. Ding, Y. Wen, H. Ju, X. Zhang, 'MicroRNA: function, detection, and bioanalysis', *Chem. Rev.* **2013**, *113*, 6207-6233.

[38] S. L. Ameres, P. D. Zamore, 'Diversifying microRNA sequence and function', *Nat. Rev. Mol. Cell Biol.* **2013**, *14*, 475-488.

[39] S. Valastyan, R. A. Weinberg, 'miR-31: a crucial overseer of tumor metastasis and other emerging roles', *Cell Cycle* **2010**, *9*, 2124-2129.

[40] E. J. Lee, M. Baek, Y. Gusev, D. J. Brackett, G. J. Nuovo, T. D. Schmittgen, 'Systematic evaluation of microRNA processing patterns in tissues, cell lines, and tumors', *RNA* **2008**, *14*, 35-42.